DESY Summer Student
Programme 2011

Using the Moon as an electron - positron Spectrometer

CTA Group, DESY Zeuthen

Aristotle University of Thessaloniki, Greece
Department of Physics

Author: Dimitris Kyriazopoulos

Supervisor: Gareth Hughes

Abstract

The project of summer students programme 2011 in DESY Zeuthen, was related with some recent advances in the field of Imaging Atmospheric Cherenkov Telescopes. The simulation of a new observation method which included moon took place, in conjuction with testing proposed observational filters and studying the ramifications to cameras.

1 Introduction

Gamma ray astronomy is a field that studies the production of relativistic particles from high energy astrophysical processes and the associated gamma radiation. The spectrum of this radiation covers an extensive range, from few MeV, until the class of TeV and even higher. This energy range can not be achieved using our current space technology, because an area of at least 100 square meters is required. For this reason, ground observations dominate in this area, which is called ground based gamma ray astronomy. The most well known source of gamma rays discovered so far, is the Crab Nebula. Crab Nebula is a supernova remnant and pulsar wind nebula which is located in the constellation of Taurus, in a distance of 2000pc. It is used as the "standard candle" in gamma ray astronomy, because it is extremely bright in gamma rays and seems to have constant flux.

Figure 1: Crab Nebula in X-rays

2 Motivation

Observations of high energy gamma rays require moonless nights, so as to lower the level of night sky backround that affects our observational data, which will yield more accurate results. However, some recent satellite observations, indicate an anomaly in the measured ratio of electrons and positrons in the flux of cosmic rays. By taking advantage of the significantly higher energy range, which can be provided by ground observations, we will be able to study the energy spectrum of the particles using the Moon.

One of the main features that encourages us to implement this new observational method, is the expected lunar shadow in both leptonic and hadronic cosmic rays. The exploitation of this effect, derives from the hole created by the moon in the flux of electrons and positrons in high energy cosmic rays. This phenonmenon is very helpful in studying the properties and the origin of cosmic rays. Furthermore, the application of observing at moonlight will be extremely helpful next year. On March 2012, the projections of Crab Nebula and Moon to Earth will be aligned. The eclipse of Crab Nebula will enable an occulation measurement, which will provide new data about Crab Nebula.

Moreover, our work is related with duty cycle of telescopes. A significant increase in the telescope overall duty cycle by a factor of 15 % is provided by taking observations at moonlight. The duty cycle is strongly dependent with the total scientific knowledge which can be provided by the telescopes and naturally with the funding of the telescope. The total number of night time without moonlight, if any weather is taken into account, is 1000 hours per year. Using filters, the duty cycle of the telescope is increased and more observations can be taken.

3 Theoretical Introduction

3.1 EAS - Cherenkov Light Emission

Whenever a very high energy cosmic or gamma ray hits at the top of the atmosphere, it interacts with the atmosphere. The result of this interaction is an extensive air shower (EAS) and its properties depend on the particle that initiated it. It is divided into 2 categories, hadronic and electromagnetic showers. In the case of hadrons, we have a massive production of gammas, electrons , positrons and hadrons. Electrons and positrons produce later gamma photons. Hadrons, mostly kaons, decay into pions ($\pi^{\pm}$, π^{o}) which produce secondary muons, electrons/positrons pairs and gammas. The production of new particles, takes place until a critical value at the energy is reached and therefore no more new particles can be created.

In case of photon though, we have the production of an electromagnetic cascade, where electrons and positrons are created. On the next step, electrons and positrons produce bremsstrahlung photons resulting to the inital condition and lose energy through ionization with the molecules of the atmosphere. This procedure yields to the development of the electromagnetic shower in the atmosphere, so the number of the electrons, positrons and photons increases by a power law as a function of atmospheric depth.

If those secondary particles move through atmosphere with speed greater than the speed of light in the medium (i.e. atmosphere) they emit radiation which is called Cherenkov Radiation or Cherenkov Light. By detecting this Cherenkov light, we are able to extract information about the original photon which occured the atmospheric shower. This detection method is called imaging atmospheric Cherenkov technique.

According to the Cherenkov effect, whenever a particle moves with a velocity (u) which is greater than the speed of light (c) for the medium of a specific refraction index (n) (in case of atmosphere, it is dependent to density), it emits Cherenkov light. The formula which represents this phenomenon is the following

$$\frac{u}{c} \geq \frac{1}{n} \Rightarrow \beta = \frac{1}{n}$$

. From the previous formula, the Cherenkov Angle can be extracted,

$$\cos(\theta_c) = \frac{1}{n * \beta}$$

which describes the angle by which the Cherenkov photons are emitted.

3.2 Electrons and Positrons in Cosmic Rays

The recent years, satellite telescopes, like PAMELA and FERMI have provided lot of information regarding the nature of very high energetic cosmic rays. PAMELA instrument is on board of Resurs-DK1 satellite [5] and has a detection area of $\sim$ 100cm^2 and it is able to measure electron flux up to 400 GeV and positron flux up to 270 GeV. FERMI [10] is a Gamma-ray Space Telescope scanning with the energy range of 10 MeV - 300 GeV and detection area $\sim$ 160cm^2. On 2011, the PAMELA Collaboration announced an apparent excess at the fluxes of positrons and electrons in cosmic rays[7]. The ratio of positrons and electrons seems to increase unexpectedly above 10GeV in conjuction with an increase of the flux of total electrons (e^+ and e^-) in the energy area of 300-800GeV observed by FERMI. An example of those measurements is shown at Figure 2.

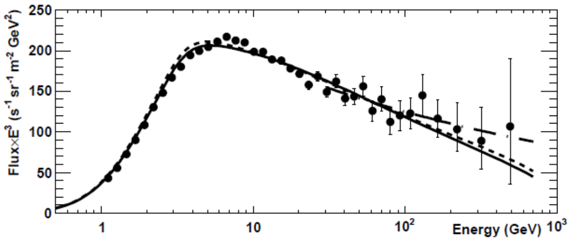

Figure 2: Comparison between PAMELA measurements and theoretical models [7]

According to the PAMELA results ([7] and [11]) , the fraction of positrons increases in a way which can not be attributed to secondary sources of cosmic rays and therefore a primary source, namely an astrophysical object, is considered to be responisble for this excess. Cosmic ray theory predicts that the energy losses of primary cosmic rays during propagation should yield a fall in the fraction of positrons as a smooth function of increasing energy. Therefore, secondary production of cosmic rays responisble for this excess should be excluded, and new explanations should be considered. Some of them, included new, not yet observed, extragalactic cosmic rays sources or nearby cosmic rays accelerator [9]. Other opinions, attribute this phenomenon to dark matter [8], on which according to cosmological models, decay of dark matter would yield γ + X or e$^+$ + X where X is an exotic particle like WIMPs.

Therefore, an accurate and precise measurement of the electrons / positrons ratio at cosmic rays is desirable. Ground observations provide us higher energy threshold and this feature can be deployed in extracting new data and discovering phenomena in the area of astroparticle physics.

3.3 VERITAS Telescope

Gamma rays astronomy is based on ground imaging atmospheric cherenkov telescopes. Nowadays, three main very high energy telescopes exist. VERITAS in USA, H.E.S.S in Namibia and MAGIC in La Palma, Canarian Islands. The work which has been conducted in this report, is related to VERITAS.

VERITAS (Very Energetic Radiation Imaging Telescope Array System)[4] is an array of 4 telescopes, 12m diameter each, located in Southern Arizona, USA. VERITAS optics are based on the Davies-Cotton design, using 350 similar hexagonal mirrors giving a total reflector area of 110 m^2. The camera is located at the focal plane which is 12 meters away from the mirrors and contains 499 pixels, 0.15^o diameter each, and has a field of view of 3.5^o. The sensitivity of VERITAS Telescope cover an energy range from $\sim$ 100 GeV to $\sim$ 30 TeV with energy resolution of 15–20%. The point source sensitivity of VERITAS is 1% of equivalent to Crab Nebula flux in less than 30h and 10% in 30 min.

Figure 3: VERITAS Array

4 Monte Carlo simulations

The observation of gamma rays is a counting experiment, but it is not 100% efficient. The number of the missed events should be calculated and for this reason, Monte Carlo simulations are being used, so as to generate more realistic situations. The software packages that were used in the simulations were the following.

- CORSIKA
  CORSIKA [12] is a simulation package of extensive air showers which are caused by high energetic cosmic ray particles. It has been developed by University of Karlsruhe, Germany, initially for KASCADE Experiment (detection of Cosmic Rays with air showers), but it is widely used for air shower simulations.

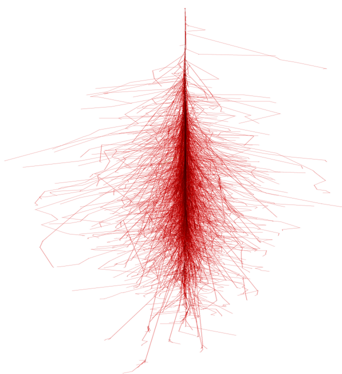

Figure 4: Shower induced by gamma ray using CORSIKA

- GrISU / CARE
  GrISU and CARE are software packages related with the procedure of collecting and analysing the light emitted from the particles. GrISU (developed by University of Utah, USA) simulates telescope response and focus to Cherenkov light produced by the shower. CARE is a software package developed by VERITAS collaboration and simulates the trigger system of the telescope.

- EVENTDISPLAY
  EVENTDISPLAY is a software package delevoped by VERITAS collaboration. The main use of the package is to parametrize images using the data taken from the trigger system and to reconstruct the events. Furthermore, having reconstructed the events, information regarding the energy of the cosmic ray which induced the shower or the integral flux of particles or plot maps, can be extract by analysing the events with EVENTDISPLAY.

5 Proposed Observation mode

5.1 Earth - Moon spectrometer system

The main reason why Earth - Moon system can be considered as spectrometer, derives from the properties of Earth magnetosphere. Whenever a particle enters the magnetosphere its trajectory is deflected, depending on charge and momentum. Therefore, the Moon creates a hole (Moon shadow) in the isotropic flux of Cosmic Rays. The missing flux is approximately 0.5^o diameter and varies of $\pm 12\%$ as a function of Moon and observer distance[3].

As it has been already mentioned, the size of Moon shadow is directly dependent on the particles charge. For neutral Cosmic Rays (like diffuse gamma rays) the shadow lies on the actual position on Moon. For charged Cosmic Rays though, the shadow is shifted perpendicularly by an angle factor $> 0.5^o$ to the geomagnetic field in an East-West axis orientation, namely for negatively charged, it is shifted eastward and for positively charged, it is shifted westward. As most of Cosmic Rays contain positive particles, Moon shadow is asymmetric with a larger deficit at the west side of the Moon. As shown in Figure 5, by exploiting the rising and falling of the Moon at different elevation angles both areas of electrons and positrons shadows can be obsereved.

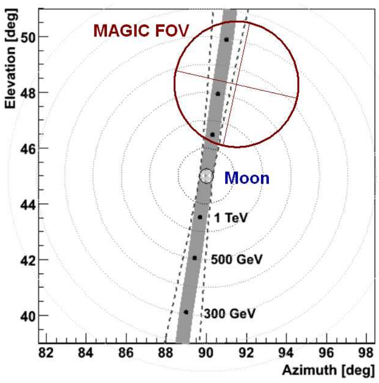

Figure 5: Positions of Moon shawdows at MAGIC Telescope. Electrons shadow is below Moon whereas positrons is above[1]

Another significant factor which is important for Moon observation, is the illumination of the Moon and the zenith angle because of the background light induced by scattering moonlight. Recent studies [3] show that the background at 3.5^o away from Moon, for half-Moon and 45^o of declination, is 40 times higher than dark sky. A small phase moon though, is rarely in sufficient elevation for observations. In that case, phase lower than 50% and zenith angle lower than 50 degrees are required. Those conditions exist only 30 hours (shared time between positrons and electrons) per year and it is located either in East ,rising before Sun, or in West, falling after sunset. Furthermore, the best period to observe electrons shadow is the beginning of the night on spring equinox and the positrons shadow at the end of night at the autumn equinox.

Even in the case that Moon is out of telescope's field of view, the induced background light will still be extreme and therefore, safe observations, meaning avoid to induce high currents in the tubes, can not be taken. Therefore, the use of ultra-violet filters is essential, because the possible observing time will be increased and observations at brighter moon phases, even closer to full moon will be feasible.

5.2 Observational Tests

One of the most significant effort made to exploit the Moon shadow effect using Cherenkov Imaging Technique, was the ARTEMIS experiment [6] in the late 90s, aiming to measure proton / antiproton ratio. The principle for this experiment, was to equip the camera of Whipple Telescope with an ultra-violet filter between 300-200nm because moonlight is absorbed by the ozone layer at these wavelengths and it would not induce background signal. This wavelength has been selected because Cherenkov light peaks in the blue / ultra-violet region , propotional to $1/\lambda^2$ until a cut-off around 300nm. Data published by the ARTEMIS experiment showed no deficit to particles shadow, but this might be due to large systematic errors. The VERITAS array however, or the future experiment Cherenkov Telescope Array (CTA) have better sensitivity which makes them ideal for Moon observation.

A recent test trying to use optical filters in moon observations was made by VERITAS on May 2011 [1]. Observations were taken using 2 types of optical filters in 2 pixels of the 499 on VERITAS Telescope camera. The filters used were Schott glass filters , BG3 and UG11. Both of them are ionically colored glasses and band pass filters. BG3 filter has a reflection coefficient of 0.92, thickness $1mm$ and density $2.56g/cm^3$. Similarly, UG11 filter has a reflection coefficient of 0.91, thickness $1mm$ and density $2.92g/cm^3$. The internal transmittance, UG11 peaks (0.99) in the region of ultra-violet $330nm$, while BG3 peaks (0.99) also in the ultra-violet $350nm$ and also in the area of infrared (770-920nm), but this area is not useful for our observations due to the quantum efficiency of the phototubes.

Furthermore, in order to calibrate the tubes, LED flashers, peaking at 375nm, were used. As shown in Figure 6, BG3 filter passes almost all LED light while UG11 cuts off at 380nm and removes a significant amount of moon spectrum. Extending those measurements to moon nights, test data was taken. According to these results, with moon's illuminated fraction 0.656, filter BG3 retains 55% of Cherenkov light and reduces the backround by a factor of 4 and filter UG11 retains 30% of Cherenkov light and reduces the backround by a factor of 12. Apart from transmittance and rejection of background, the cost of the filters is of interest. For a $36cm^2$ filter, BG3 costs €140 and UG11 costs €450 [1]

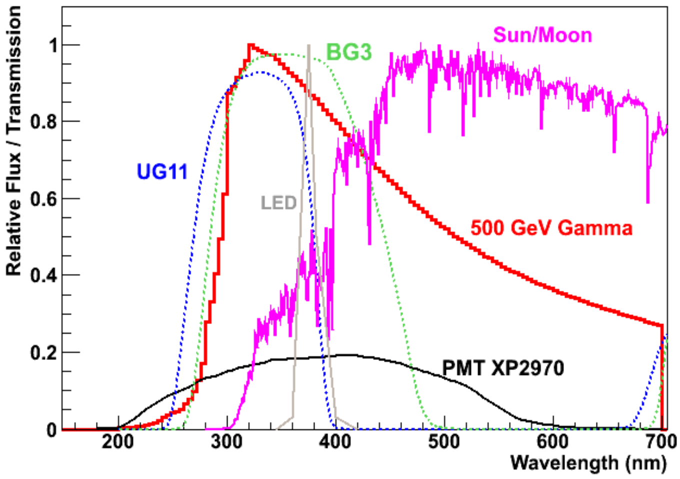

Figure 6: Transmission of filters used in VERITAS tests

6 Filter simulations

The main idea of the simulations was to extend the previous VERITAS test by simulating the case that all of 4 Telescopes cameras (499 pixels - PMTs each) have been equipped with ultra-violet filters (BG3 and UG11). To conduct those experiments, 3 programmes were used, CARE and EVENTDISPLAY related with simulating electronics and ROOT for data analysis. The CORSIKA/GrISU configuration files needed for the simulation, were provided by VERITAS collaboration.

6.1 Noise level calculation

Primarily, in order to conduct accurate simulations, the quantum efficiency and the behaviour of PMTs is needed. Data for this procedure, were taken by the previous VERITAS observational test, namely, the quantum efficiency of the PMTs without any filters and the transmission of the filters. By convolving the transmission of the filters with the quantum efficiency of the PMTs, the behaviour of the tubes with filters installed was simulated.

The next step was to reproduce the night sky background with which the VERITAS tests took place. For this reason, further analysis of test data was made by associating the variance of pedestal (pedvar) with the frequency of night sky background (NSB). The pedestal is the value of the output signal of the PMTs, when no Cherenkov light is detected. It is a value which plays a significant role in quantifying and recording the noise to each PMT. Reproduction of VERITAS test was done by calculating the mean value of pedvars for the telescopes for a range of frequencies which resembled arbitary values of night sky background. Next, having calculated mean pedvars, those values were compared with the actual mean pedvars values given by VERITAS trigger system. Our analysis concluded that the night sky background at test date, for UG11 and BG3 filters was 15 MHz and 60 MHz respectively.

6.2 CARE simulations

The level of night sky background for each of the filters (15 MHz and 60 MHz) and without filters (110 MHz and 1000 MHz, as a control) were inserted as input arguments to CARE so as to generate the trigger situation. The topological details for the simulations were, telescope azimuth 20.0 degrees with a wobble of 0.5 degrees. The wobble value is related with the acceptance of camera and it is established so as to prevent systematics errors. CARE produced 100 data files for every night sky background containing 10000 events each, including trigger infomartion and energy levels. Afterwards, those files were merged and on the next analysed and being reconstructed by EVENTDISPLAY which calculates the arrival direction of the initial gamma-ray.

6.3 Reconstrunction of events with EVENTDISPLAY

Proper reconstruction of events require the pedestal for each event should be calculated. Having this value established, EVENTDISPLAY[2] loops over the events contained to the raw data files, from the simulations. For each single event, specific cuts are taken into account so as to reject weak triggered events. Weak triggered events derive from weak light flux, as a result of that, those events are bad reconstructed and have bad resolution, so, they should be rejected. Furthermore, in case of signal, the calculation of the mean scaled length and width takes place so as to separate the origin of the events. Images with a well formed oval shape resemble to gamma ray showers, as shown on Figure 7(a) and 8(a) , while badly formed images represent hadronic showers, Figure 7(b), since we have then the creation of numerous particles. Afterwards, in each events, combining the data from every telescope EVENTDISPLAY, calculates the arrival direction of initial gamma ray as shown on Figure 9(a) and 9(b).

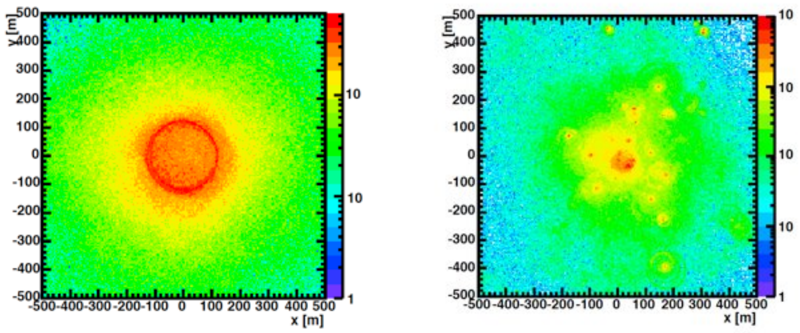

(a) (b)

Figure 7: Distribution of Cherenkov light on the ground from a Gamma Ray event(a) and a proton shower(b)

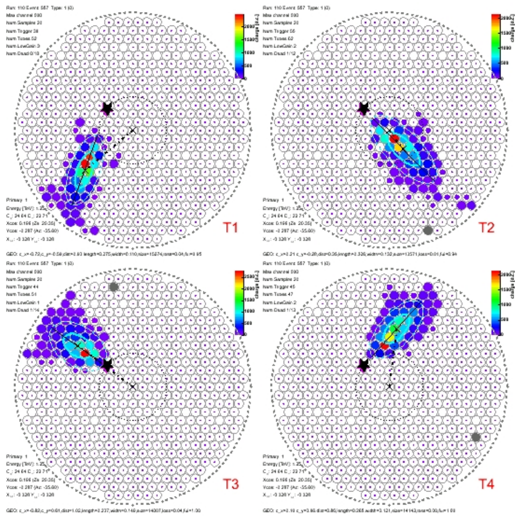

(a)

Figure 8: Image Reconstruction on EVENTDISPLAY

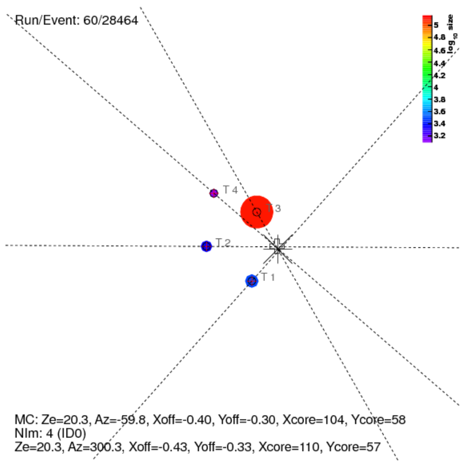

(a)

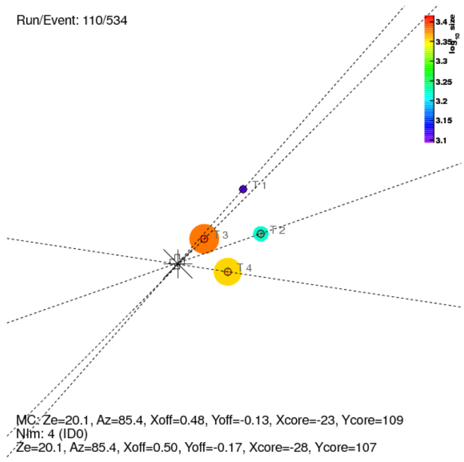

(b)

Figure 9: Reconstruction of events. Cross represents the impact point in the ground and circles around telescopes represent the amount of light collected by each telescope.

After the reconstrunction of the events, EVENTDISPLAY generates the table files. Those root files, contain information for the energy levels of the events. Using those tables files, the simulation procedure continues with the calculation of the effective area of the events.

The effective area is the result of simulations. Effective area describes the number of total reconstructed events N_{REC} divided by the Monte Carlo thrown events N_{MC} and multipled by the scattered area A_{MC}.

$$A_{eff} = \frac{N_{REC}}{N_{MC}} * A_{MC}$$

EVENTDISPLAY calculated the effective areas and associated them with the energy under which telescope operates and by fitting the energy threshold is calculated.

7 Results

To get the effective areas, 2 different types of cuts have been implemented to the data. Those cuts are related mainly with angular resolution, length, width and angle of the shower cone. At first step we applied moderate cuts to these parameters and as a second step, since diffuse electrons and positrons can not be considered as a point like source, the θ^2 value increased from 0.01 to 0.1. The θ^2 value is the angular distance between arrival direction of shower and source location. This happened because the main goal of this analysis is to produce higher effective areas with lower energy threshold.

Analysising of our data, EVENTDISPLAY yielded the following plots for the effective areas.

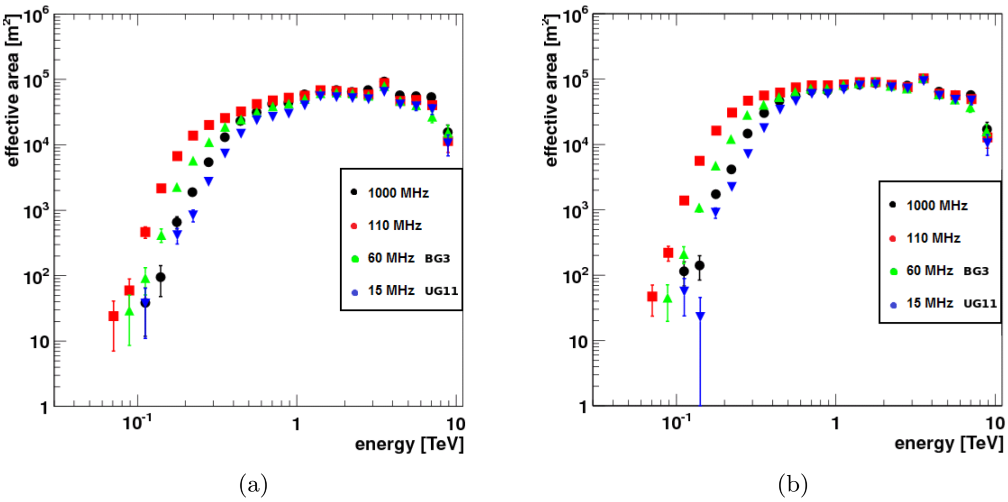

Figure 10: Using moderate cuts (a) , and $\theta^2 = 0.1$(b)

Interpreting the plot, it is observable using filters the energy uder which telescope operates, changes. Therefore, an energy threshold for telescope operation should be established. The main goal is to have low energy thresholds with high effective areas. According to our results it seems that energy threshold with filter remains below TeV which yields a good energy coverage of observations.

On the final step, using EVENTDISPLAY we took the plateau of the effective areas, reduced it by 20% and the value of energy for this fitted effective area point is the energy threshold. By applying this method, the following results were extracted.

Filter	NSB (MHz)	Cut	Threshold (GeV)
UG11	15	Mod	446.68
UG11	15	θ^2	354.81
BG3	60	Mod	281.84
BG3	60	θ^2	281.83
no	110	Mod	223.87
no	110	θ^2	223.87
no	1000	Mod	448.7
no	1000	θ^2	281.83

Comparing the energy thresholds for the different filters, it is noticable that BG3 filter has the lowest energy threshold in both cuts methods. In moderate cuts, UG11 has a higher energy threshold than 110MHz NSB without any filter. BG3 threshold, however, is lower than UG11 and a bit higher than 110MHz. This difference implies that BG3 could potentially be better for full moon observations.

Furthermore, the implementation of θ^2 cut, showed no change to BG3 threshold, lowered UG11 threshold but still it remains higher than BG3. Also, it is should be mentioned that, the new cut did not change the energy threshold of telescope at 110MHz NSB, and lowered it at 1000MHz.

Since BG3 seems to have the lowest energy threshold, we wanted to extent the simulation, from half Moon (according to VERITAS test conditions), to full moon. For this reason, assuming that Moon had a small ($\sim 5^o$) angle with horizon, and telescope pointing to zenith, we multiplied by a factor of 20, so as to recreate a condition where the relative angle between telescope and full moon is small. The result was 1200MHz which represents a $\sim$ 85% full Moon.

By inputing those parameters to CARE and following the same simulations procedure as before, EVENTDISPLAY extracted the following effective areas plot.

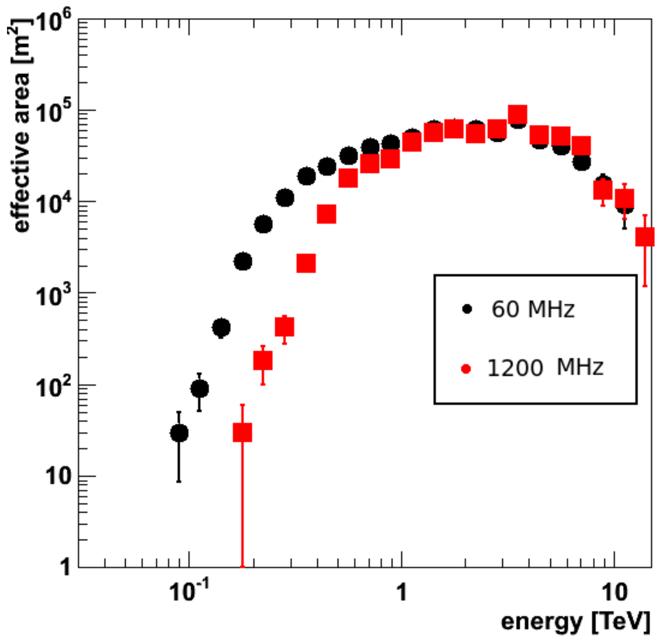

Figure 11: Effective areas for BG3 filter at 60 and 1200MHz night sky background

The energy threshold calculation yielded the following results

Filter	NSB (MHz)	Cut	Threshold (GeV)
BG3	60	Mod	281.84
BG3	60	θ^2	281.83
BG3	1200	Mod	562.34
BG3	1200	θ^2	446.68

Interprating the previous results, the energy threshold of the telescope, using BG3 filter does not seem to increase in a very high extent. Even in the case of moderate cuts, an energy threshold of $\sim$ 500 GeV is sufficient for safe high phase moon observations.

8 Conclusion

The analysis of the simulations data yielded some really interesting results. First of all, both UG11 and BG3 filters are appropriate for $\sim$ 60% of Moon illuminating, since the energy thresholds are on the band of safe observations. Selecting BG3 as a filter which could potentially be used for full moon observations, due to its lowest energy threshold, the final result showed that even in that case, the energy threshold remains low. Assuming a similar behaviour, UG11 should not have an energy threshold which could hinder us from using it to full moon observation. Even though BG3 seems better in terms of energy, observations with BG3 would have more background light since it reduces background by a factor of 4, comparing to UG11 reduces background by 12 times. Also, according to Figure 5, BG3 filter is better for flasher calibration of the telescope, since it passes all of the LED light. Finally, selecting a filter for observations someone should definetely take into account the cost, since $\sim$ €100,000 - 200,000 are needed to equip all the 4 VERITAS Telescopes with each type of filter , namely BG3 and UG11.

9 Acknowledgements

There are many people who I would like to thank for this summer experience here in DESY Zeuthen. First of all, I am really grateful to Stefan Schlenstedt and Gernot Maier, for giving me the chance to work in the CTA Group and having the chance to experience real research. Also, I have to thank Karl Jansen and Sabine Baer for the excellent coordination of the programme and their honest efforts to make us feel comfortable every time here.

Next, I would like to thank my supervisor, Gareth Hughes, for all the great cooperation we had this summer. He was really patient and willing to answer all of my questions, something which I really appreciated. Furthermore, I have to thank my office-mates, Heike Prokoph, Christian Skole and Guillaume Decerprit, for their precious help, advices and helpful comments regarding my work.

In addition, I would like to express my thanks to my professors in Thessaloniki, K. Kordas and D. Sampsonidis, for the encouragment and perparation for the programme.

Finally, I am mostly grateful to my family. All their support, courage and advices were really vital for me during this summer period.

$\Sigma\alpha\varsigma\ \epsilon\upsilon\chi\alpha\rho\iota\sigma\tau\omega\ \pi o\lambda\upsilon$!

Email: dkyriazo@physics.auth.gr

References

[1] J. Holder, Summary of Optical Filter Tests, VERITAS Internal Note, May 2011

[2] R. Guenette, VERITAS observations of galactic compact objects, Ph.D. Thesis ,McGill University (Canada), 2010. AAT NR72634

[3] P. Colin *et al.*, arXiv:0907.1026 [astro-ph.IM].

[4] J. Holder *et al.* [VERITAS Collaboration], Astropart. Phys. **25**, 391 (2006) [arXiv:astro-ph/0604119].

[5] S. Orsi [PAMELA Collaboration], Nucl. Instrum. Meth. A **580**, 880 (2007).

[6] D. Pomarede *et al.*, Nucl. Instrum. Meth. A **446**, 469 (2000).

[7] O. Adriani *et al.* [PAMELA Collaboration], Phys. Rev. Lett. **106**, 201101 (2011) [arXiv:1103.2880 [astro-ph.HE]].

[8] A. Ibarra and D. Tran, JCAP **0902**, 021 (2009) [arXiv:0811.1555 [hep-ph]].

[9] P. Mertsch and S. Sarkar, arXiv:1108.1753 [astro-ph.HE].

[10] M. Ackermann *et al.* [Fermi LAT Collaboration], Phys. Rev. D **82**, 092004 (2010) [arXiv:1008.3999 [astro-ph.HE]].

[11] O. Adriani *et al.* Nature 458, 607-609 (2009)

[12] D. Heck, G. Schatz, T. Thouw, J. Knapp and J. N. Capdevielle, FZKA-6019, (1998)